

Figure 1. Rise (r) and decay (f) of chemiluminescence for reaction of [TCPO] = 0.5 mM; [DPA] = 0.25 mM; [H₂O₂] = 5.0 mM and [imidazole] = 2.5 mM at pH = 7.0 and 25 °C in 75% (aqueous) acetonitrile.

burst in aqueous media emerges as being determined by only three readily measured parameters. We present these quantities as functions of reaction conditions and derive a mechanistic model for the reaction.

Experimental Section

Chemiluminescence. Chemiluminescence (CL) experiments were carried out in the chemiluminescence monitoring instrument (CMI) designed and constructed by the Instrument Design Laboratory at University of Kansas. The apparatus consists of the monochromator, detector, and sample modules of a GCA/McPherson spectrophotometer assembled according to the design described by Catherall et al.³ The emission was monitored at 430 nm, the fluorescence maximum of 9,10-diphenylanthracene (DPA). The total output of the chemiluminescence system was determined by potassium ferrioxalate actinometry⁵ and by comparison with the intensity of the chemiluminescence reaction of the standard luminol reaction of known chemiluminescence quantum efficiency.^{6,7} The reaction cell was maintained at a constant temperature by circulating water through the cell compartment from an Endocal RTE-9 constant-temperature water bath.

Materials and Solutions. Stock solutions of bis(2,4,6-trichlorophenyl) oxalate (Fluka AG, CH-9470 Buchs, [TCPO] = 1.0 mM) and 9,10-diphenylanthracene (Sigma, D-3519, [DPA] = 1.0 mM) were prepared in acetonitrile (Fisher Scientific, HPLC grade). Hydrogen peroxide solutions (Fisher Scientific, H325) were used as 30% and 3% aqueous solutions. The imidazole buffers were prepared with either hydrochloric or sulfuric acid addition to imidazole (Sigma, I-0250) in concentrations of 10, 20, and 40 mM at pH 7.0 and 7.5. The solutions were transferred with either a Gilson Pipetman, a Pharmaseal 1-mL syringe, or a Hamilton microliter syringe. For a typical CL run, 1.0 mL of 1.0 mM TCPO and 0.5 mL of 1.0 mM DPA solutions in acetonitrile were mixed in a 1 × 1 cm cuvette which was placed in the CMI. Next, 0.5 mL of a mixture of imidazole buffer and 3–6 μL of hydrogen peroxide were transferred to a 1-mL thermostatted syringe. After the temperature of the imidazole-hydrogen peroxide solution had reached equilibrium, the solution was rapidly injected into the cuvette, initiating the CL reaction. The solvent composition of the final solution was 75% acetonitrile and 25% water by volume. Data collection was initiated simultaneously with the injection of the imidazole-H₂O₂ solution.

Kinetics. The emission from a typical oxalate reaction in aqueous solutions exhibited a characteristic light intensity/time

Table I. Effect of the TCPO Concentration on the Rise (r) and Fall (f) Rate Constants, τ_{\max} , the Maximum Intensity (J), and the Quantum Efficiency (Φ_{CL}) in the Peroxyoxalate CL Reaction^a Conducted in 75% Aqueous Acetonitrile (Error Limits from Analysis of Three or More Determinations Are Given in Parentheses)

[TCPO], mM	r , s ⁻¹	$10^2 f$, s ⁻¹	τ_{\max} , s	J , au	$10^4 \Phi_{\text{CL}}$, E
[H ₂ O ₂] = 5.0 mM					
0.5	0.99 (0.04)	3.15 (0.37)	2.5	6.7 (0.4)	18.30 (3.16)
0.375	0.71 (0.12)	2.98 (0.51)	3.1	6.1 (0.3)	16.17 (0.18)
0.25	0.94 (0.05)	3.29 (0.17)	2.8	4.8 (0.6)	10.57 (1.41)
0.188	0.86 (0.09)	3.40 (0.04)	2.5	3.7 (0.3)	8.97 (0.84)
0.125	0.95 (0.04)	4.09 (0.37)	3.0	3.0 (0.2)	6.24 (0.98)
0.094	0.93 (0.04)	3.41 (0.07)	2.5	2.3 (0.1)	5.34 (1.23)
0.063	1.01 (0.06)	4.14 (0.41)	2.5	1.7 (0.4)	3.66 (0.38)
0.047	0.95 (0.06)	3.60 (0.07)	2.8	1.2 (0.1)	2.90 (0.23)
0.031	0.79 (0.04)	4.34 (0.10)		1.1 (0.1)	2.39 (0.14)
[H ₂ O ₂] = 30.0 mM					
0.500	1.91 (0.11)	3.02 (0.30)	1.5	9.6 (2.5)	20.13 (0.86)
0.375	2.08 (0.07)	3.07 (0.29)	1.5	9.1 (2.8)	16.32 (0.14)
0.250	2.17 (0.05)	3.98 (0.35)	1.4	6.2 (0.1)	11.99 (0.87)
0.188	1.85 (0.07)	3.25 (0.09)	1.5	4.2 (0.5)	8.49 (0.48)
0.125	2.13 (0.10)	4.53 (0.56)	1.5	3.7 (0.1)	
0.094	1.81 (0.07)	3.54 (0.06)	1.5	2.7 (0.5)	5.25 (0.48)
0.063	2.00 (0.18)	3.21 (0.21)	1.5	2.1 (0.1)	4.04 (0.30)
0.047		3.68 (0.05)	1.3	1.5 (0.1)	3.24 (0.27)
0.031		4.34 (0.62)	1.5	1.1 (0.2)	2.25 (0.12)
0.016			1.4	0.6 (0.1)	1.41 (0.15)

^a [DPA] = 0.25 mM, [imidazole] = 2.5 mM at pH = 7.0 and 25 °C.

profile of a simple rise and fall as shown in (Figure 1). The data are most easily interpreted if the reaction profile is considered as separate rise and fall stages. One model for the observed profile takes the form of the consecutive sequence of the irreversible pseudo-first-order transformation.⁸ Two pseudo-first-order rate constants, r for the rise and f for the decay of the intensity/time (I_t) emission profile, were then calculated by weighted nonlinear least-squares analyses, commonly using 50 to 300 data points. The reported rate constants are the mean of three to seven independent measurements for these two regions. Other important reaction characteristics are the time required to reach maximum intensity (τ_{\max}), the intensity at the maximum (J), and the total quantum efficiency (Φ), which is directly proportional to the area under the I_t chemiluminescence profile.

Results

Variation of the TCPO Concentration with Excess Hydrogen Peroxide. The data presented in Table I show the effect on r , f , τ_{\max} , J , and Φ_{CL} of varying the TCPO concentration when imidazole buffer and fluorophore concentrations are constant and hydrogen peroxide is either 5.0 mM or 30.0 mM in 75% aqueous acetonitrile at pH 7.0 and 25 °C.⁹ The data show that the pseudo-first-order decay rate constants r and f are independent of TCPO concentrations (Table I). Similarly, the time required to reach maximum intensity (τ_{\max}) does not show TCPO dependence when the hydrogen peroxide concentration is in moderate excess. The total quantum efficiency (Φ_{CL}) increases in direct proportion to the TCPO concentration, whereas J appears to be a complex function of the TCPO and H₂O₂ concentrations.

Variation of Hydrogen Peroxide Concentration. The data presented in Table II show the effect on r , f , J , and Φ_{CL} of varying the hydrogen peroxide concentration

(5) Hatchard, C. G.; Parker, C. A. *Proc. R. Soc. London, Ser. A* **1956**, *235*, 518.

(6) Melhuish, W. H. *J. Phys. Chem.* **1960**, *64*, 762.

(7) Parker, C. A. *Photoluminescence of Solutions*; Elsevier: New York, 1968; p 252.

(8) Laidler, K. J. *Chemical Kinetics*, 3rd ed.; Harper and Row: Cambridge, 1987; pp 279–281.

(9) Acetonitrile solutions of TCPO were found to be stable for several weeks. However, in aqueous acetonitrile mixed solvents ([H₂O] = 1.6 M), TCPO reacted with a rate constant for decomposition of $k = 7.15 \times 10^{-6}$ s⁻¹ and a half-life ($t_{1/2}$) of 26.9 h.

Table II. Effect of the Hydrogen Peroxide Concentration on the Rise (r) and Fall (f) Rate Constants, the Maximum Intensity (J), and the Quantum Efficiency (Φ_{CL}) in Peroxyoxalate Chemiluminescence in 75% Aqueous Acetonitrile^a (Error Range Is Given in Parentheses)

[H ₂ O ₂], mM	r , s ⁻¹	10 ² f , s ⁻¹	J , au	10 ⁴ Φ , E
1.25		3.42 (0.20)	3.8 (0.2)	7.08 (0.17)
2.5	0.72 (0.04)	3.57 (0.15)	5.4 (0.1)	9.14 (0.29)
5.0	1.04 (0.08)	3.16 (0.23)	6.9 (0.3)	11.83 (1.09)
10.0	1.20 (0.02)	3.29 (0.18)	7.9 (0.4)	12.72 (0.89)
30.0	2.03 (0.18)	3.12 (0.47)	8.7 (0.8)	13.37 (0.74)
60.0		4.34 (0.61)	9.6 (0.4)	11.29 (0.37)
120.0		6.29 (0.76)	9.8 (0.8)	8.11 (0.59)

^a[TCPO] = 0.50 mM; [DPA] = 0.25 mM; [imidazole] = 2.5 mM; pH = 7.0 at 25 °C.

Table III. Effect of DPA Concentration on the Rise (r) and Fall (f) Rate Constants, the Maximum Intensity (J), and the Quantum Efficiencies (Φ_{CL}) in the Peroxyoxalate Chemiluminescence Reaction in 75% Aqueous Acetonitrile^a (Error Range Is Given in Parentheses)

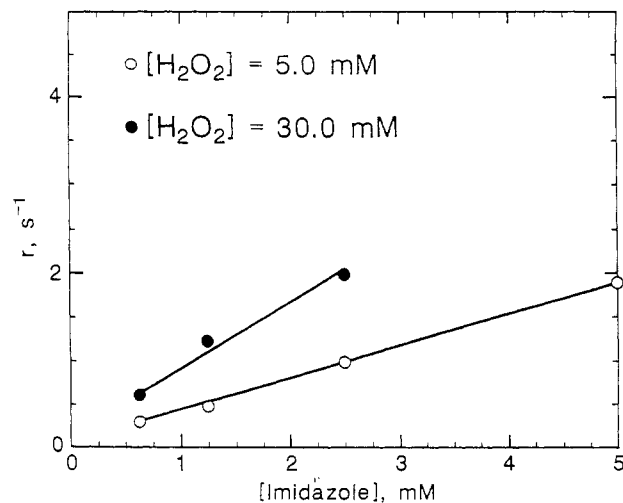
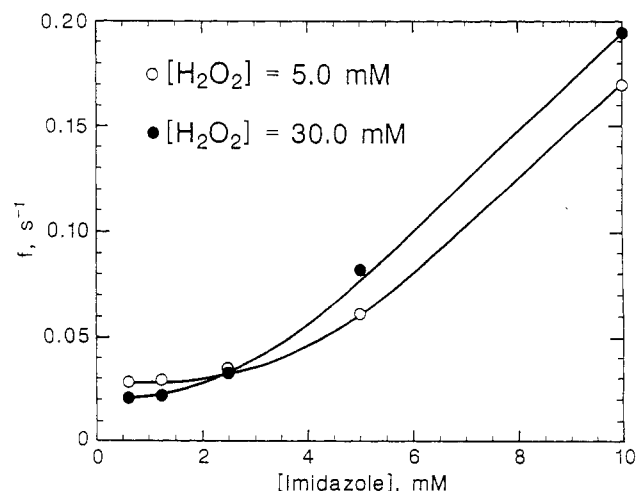
[DPA], mM	r , s ⁻¹	10 ² f , s ⁻¹	J , au	10 ⁴ Φ , E
[H ₂ O ₂] = 5.0 mM				
0.25	1.19 (0.10)	3.44 (0.10)	7.0 (0.4)	12.20 (0.52)
0.125	1.27 (0.18)	3.33 (0.09)	4.2 (0.2)	6.61 (0.35)
0.0625	1.19 (0.09)	3.32 (0.17)	2.2 (0.2)	3.45 (0.08)
0.0313	1.41 (0.27)	3.57 (0.43)	1.2 (0.1)	1.98 (0.10)
0.0156		3.62 (0.06)	0.65 (0.05)	1.16 (0.02)
0.0078		3.65 (0.03)	0.34 (0.03)	0.706 (0.01)
[H ₂ O ₂] = 30.0 mM				
0.25	2.31 (0.21)	4.04 (0.12)	9.6 (0.8)	11.9 (0.29)
0.125	2.18 (0.32)	3.57 (0.37)	4.9 (0.3)	6.54 (0.27)
0.0625	2.34 (0.29)	3.51 (0.29)	2.7 (0.1)	3.25 (0.35)
0.0313	2.46 (0.31)	3.50 (0.37)	1.4 (0.1)	1.99 (0.02)
0.0156		3.65 (0.09)	0.8 (0.1)	1.22 (0.04)
0.0078		4.37 (0.10)	0.43 (0.03)	0.72 (0.01)

^a[TCPO] = 0.5 mM; [imidazole] = 2.5 mM; pH = 7.0 at 25 °C.

when the concentrations of TCPO, DPA, and imidazole buffer are held constant at the levels given in the table. The rise rate constant (r) for the chemiluminescence emission shows a modest increase with increasing H₂O₂ concentration. The fall rate constant (f) is not dependent on the H₂O₂ concentration when there is only a moderate excess of hydrogen peroxide relative to the oxalate. At high H₂O₂ concentrations, f increases rapidly with further increases in H₂O₂ concentrations. The maximum intensity J also increases with increases in the concentration of hydrogen peroxide. However, the increase in J is not directly proportional to the increase in H₂O₂. The chemiluminescence quantum efficiency increases with increasing H₂O₂ concentration and reaches a maximum at approximately 30.0 mM H₂O₂, a 60-fold excess relative to TCPO.

Effect of DPA. The effect of variation of the DPA concentration on CL reaction is given in Table III. The rise and fall rate constants (r and f) were independent of the DPA concentration. Both the chemiluminescence quantum efficiency and the maximum intensity increased in direct proportion to increasing DPA concentration.

Variation of the Imidazole Buffer Concentration. The effect of the imidazole buffer on the rate constants, the maximum intensity, and quantum efficiency are presented in Table IV. Figures 2 and 3 graphically illustrate the dependence of r and f on the imidazole concentration. The data show that both rate constants increase with increasing imidazole buffer concentration. However, the hydrogen peroxide concentration influences the rise rate constant dependence on the imidazole concentration, i.e., at higher H₂O₂, the rise rate constant is more sensitive to the imidazole concentration. The in-

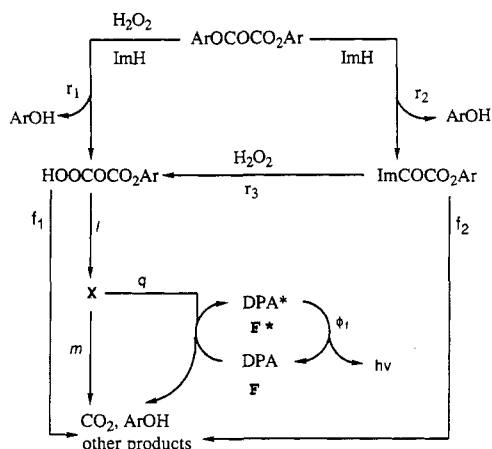
**Figure 2.** Effect of imidazole buffer concentration on the rise rate constant (r) at a constant [TCPO] = 0.5 mM and [DPA] = 0.25 mM at pH = 7.0 at 25 °C.**Figure 3.** Effect of imidazole buffer concentration on the fall rate constant (f) at a constant [TCPO] = 0.5 mM and [DPA] = 0.25 mM at pH = 7.0 at 25 °C.**Table IV. Effect of Imidazole Buffer Concentration on the Rise (r) and Fall (f) Rate Constants, the Maximum Intensity (J), and the Quantum Efficiency (Φ_{CL}) in 75% Aqueous Acetonitrile^a (Error Range Is Given in Parentheses)**

[imidazole], mM	r , s ⁻¹	10 ² f , s ⁻¹	J , au	10 ⁴ Φ , E
[H ₂ O ₂] = 5.0 mM				
10.0	8.34 (1.12)	17.10 (2.79)	9.9 (0.2)	7.15 (0.77)
5.0	1.89 (0.09)	6.12 (0.63)	9.4 (0.3)	12.48 (1.41)
2.5	0.99 (0.03)	3.48 (0.25)	7.4 (0.7)	13.51 (2.36)
1.25	0.47 (0.01)	2.97 (0.10)	4.2 (0.5)	9.84 (0.62)
0.625	0.29 (0.01)	2.83 (0.08)	2.1 (0.1)	4.59 (0.30)
[H ₂ O ₂] = 30.0 mM				
10.0		19.49 (0.71)	11.1 (0.3)	4.55 (0.06)
5.0		8.21 (0.44)	10.5 (0.2)	10.24 (0.81)
2.5	2.03 (0.17)	3.36 (0.60)	8.8 (1.7)	14.37 (1.71)
1.25	1.20 (0.05)	2.19 (0.02)	7.6 (0.4)	18.68 (0.06)
0.625	0.60 (0.02)	2.09 (0.03)	4.3 (0.1)	12.59 (0.54)

^a[TCPO] = 0.5 mM; [DPA] = 0.25 mM; pH = 7.0 at 25 °C.

tensity maximum J approaches an upper limit between 5.0 and 10.00 mM imidazole, whereas the chemiluminescence quantum efficiency reaches a maximum at a lower concentration depending on the hydrogen peroxide concentration.

Scheme II. Peroxyoxalate Chemiluminescence Mechanism



Discussion

One of the most fascinating questions concerning the peroxyoxalate chemiluminescence reaction is the structure of the compound capable of generating the excited states of DPA and related fluorophores. The hypothetical structures reported to date have been based on analogy with the dioxetane and, more recently, dioxetanone chemistry. While the analogy of cyclic peroxides may, indeed, eventually prove to be correct, the evidence to date does not exclude several other possibilities. The results of Catherall et al.³ and our previous results for the peroxyoxalate reaction using nonaqueous solvents⁴ clearly indicate the need for further investigation of the reaction mechanism.

We have addressed the question of the structures of the reactive intermediates (these intermediates are collectively termed X in Scheme II) from several approaches and herein report the results of a kinetic approach, which gives some detail on the nature of X, including the reactions leading to its formation and the routes for its decomposition. Previous stopped-flow studies showed that imidazole was an excellent catalyst for the TCPO/H₂O₂ reaction, much better than a variety of alternative amine catalysts studied.¹⁰

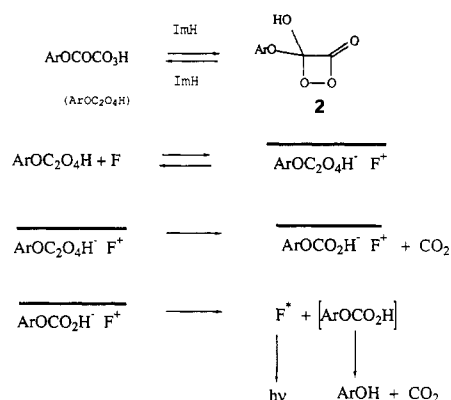
The data presented in Tables I-IV and Figures 1-3 are consistent with the mechanistic model shown in Scheme II, which is a simplified and structurally more detailed version of a previous model we presented in a preliminary communication⁴ dealing with the reaction in nonaqueous media. The model of Scheme II is given in detail in the Appendix. From this, the kinetic law of eq 1 can be derived, if the parameters r_3 and f_2 are taken to be large relative to the parameter r_2 , i.e., $r = r_1 + r_2$ and $f = f_1 + l$. The high reactivity characteristic of acylimidazoles in aqueous media justifies this constraint. I_t , the time-dependent chemiluminescence intensity, is given below:

$$I_t = \frac{d(h\nu)}{dt} = \frac{Mr}{r-f}(e^{-ft} - e^{-rt}) \quad (1)$$

where M is the maximum concentration of the reactive intermediates as defined in eq 2, where l , m , q , r_1 , r_2 , r_3 , $M = [\text{oxalate}]_0[lq\Phi_F/(m+q)][r_1 + (r_2r_3/(r_3+f_2))]$ (2)

f_1 , and f_2 are the rate constants for the individual steps in Scheme II and Φ_F is the fluorescence efficiency of the acceptor, DPA (diphenylanthracene, $\Phi_F = 1.00$). r and f are the composite rise and fall rate constants for the

Scheme III. Hypothetical Mechanism for Fluorophore Activation by Aryl Peroxyoxalates



time/intensity profile. Approximate values for the composite rate constants r and f can be determined by fitting eq 1 to the intensity/time profile of Figure 1 by a nonlinear least-squares approach.

To derive the model of Scheme II from the data in the Results section, we have outlined a possible route and described the kinetics for the conversion of the oxalate ester to reaction intermediates, at least some of which are capable of leading to the generation of light. Imidazole plays a pivotal role by catalyzing the conversion of the oxalate to peroxyoxalate. Figure 2 shows that r describes two parallel processes, both first order in oxalate ester and both first order in imidazole buffer. One of these processes is first order in hydrogen peroxide, the other is zero order in hydrogen peroxide. We propose that the first of these terms is r_1 and describes general base-catalyzed reaction of H₂O₂ with the oxalate ester to produce HOOCOCOOAr; the second would then be r_2 , the nucleophilic reaction of imidazole (ImH) with oxalate to produce ImCOCOOAr. In rapid reactions, ImCOCOOAr then decomposes to generate products or to produce, by reaction with H₂O₂, HOOCOCOOAr.

We suggest that the parameter f consists of $f_1 + l$, the former leading from HOOCOCOOAr to products along a nonchemiluminescent route, the latter to an intermediate of still unknown structure, denoted X. This intermediate is envisioned as possibly decomposing along a nonchemiluminescent route but also by interaction with the fluorophore DPA, leading to the singlet excited state, DPA*, from which the observed chemiluminescence is known to arise. Figure 3 shows that f has terms that are zero order and second order in imidazole buffer. Reactions of esters that are second order in imidazole in aqueous solution have been observed by Kirsch and Jencks.¹¹ All kinetic parameters including f are independent of the concentration of DPA.

The conversion of peroxyoxalate to X is unusual, specifically producing materials capable of reacting rapidly with DPA to generate DPA*. For example, processes such as that of Scheme III may be considered, although at present they remain hypothetical. The critical intermediate 2 is reminiscent of that suggested by Catherall et al.³ for a similar reaction of bis(pentachlorophenyl) oxalate in chlorobenzene. This adduct is one possible structure for X, which could react rapidly with DPA as indicated to produce DPA*. Reaction of X with DPA must be rapid since all rate parameters are zero order in DPA.

While the mechanistic details of the reaction of hydrogen peroxide, TCPO, imidazole, and a fluorophore have not

(10) Hanaoka, N.; Givens, R. S.; Schowen, R. L.; Kuwana, T. *Anal. Chem.* 1988, 60, 2193.

(11) Kirsch, J. F.; Jencks, W. P. *J. Am. Chem. Soc.* 1964, 86, 833.

been completely elucidated, this study has revealed several interesting and unusual features of the chemical transformations leading to the unknown intermediate (or intermediates). Continuing studies on this reaction, including the effects of temperature and the nature of the fluorophore, are in progress and promise to provide addition detail on their structure and reactivity.

Acknowledgment. We thank the Kansas Technology Exchange Commission and Oread Laboratories, Inc., for support of this research. We also thank Drs. Jeffery Bibbs and Ken Ratzlaff and Mr. David Heitmeyer for technical assistance.

Appendix. Details of the Peroxyoxalate Chemiluminescence Mechanism Shown in Scheme II

If r_3 and f_2 are large,

$$\frac{d(h\nu)}{dt} = I = \frac{Mr}{f-r}(e^{-rt} - e^{-ft}) = \frac{M}{r-f}(e^{-ft} - e^{-rt}) \quad (1)$$

where $M = [\text{OX}_0] \left\{ \left(\frac{lq\Phi_f}{m+q} \right) \left(r_1 + \frac{r_2r_3}{r_3+f_2} \right) \right\}$, $r = r_1 + r_2 = [\text{H}_2\text{O}_2](a + b[\text{Im}])$, and $f = f_1 + l = \alpha + \beta[\text{Im}] + \gamma[\text{Im}]^2$
 $[\text{OX}] = [\text{OX}_0]e^{-(r_1+r_2)t} = [\text{OX}_0]e^{-\rho t}$ $\rho = r_1 + r_2$ (2)

$$\frac{dA}{dt} = r_2[\text{OX}_0]e^{-\rho t} - (r_3 + f_2)A \quad (3)$$

where $A = [\text{ImCOCO}_2\text{Ar}]$

$$\frac{dA}{dt} + (r_3 + f_2)A = r_2[\text{OX}_0]e^{-\rho t} \quad (4)$$

$$A = \frac{r_2[\text{OX}_0]}{r_3 + f_2 - \rho} \{e^{-\rho t} - e^{-(r_3+f_2)t}\} \quad (5)$$

$$\frac{dB}{dt} = r_1[\text{OX}_0]e^{-\rho t} + r_3A - (f_1 + l)B \quad (6)$$

where B is the aryl peroxyoxalate half ester ($\text{ArO}(\text{O}=\text{C})\text{CO}_2\text{H}$),

$$\frac{dB}{dt} + (f_1 + l)B = r_1[\text{OX}_0]e^{-\rho t} + \frac{r_3r_2[\text{OX}_0]}{r_3 + f_2 - \rho}e^{-\rho t} - \frac{r_3r_2[\text{OX}_0]}{r_3 + f_2 - \rho}e^{-(r_3+f_2)t} \quad (7)$$

$$\frac{dB}{dt} + (f_1 + l)B = [\text{OX}_0] \left[r_1 + \frac{r_2r_3}{r_3 + f_2 - \rho} \right] e^{-\rho t} - \frac{r_2r_3[\text{OX}_0]}{r_3 + f_2 - \rho} e^{-(r_3+f_2)t} \quad (8)$$

$$B = \frac{[\text{OX}_0] \left[(r_1 + r_2)r_3 + r_1f_2 - r_1\rho \right]}{(f_1 + l - \rho)(r_3 + f_2 - \rho)} \{e^{-\rho t} - e^{-(f_1+l)t}\} - \frac{[\text{OX}_0](r_1r_3)}{(f_1 + l - r_3 - f_2)(r_3 + f_2 - \rho)} \{e^{-(r_3+f_2)t} - e^{-(f_1+l)t}\} \quad (9)$$

$$\frac{B}{[\text{OX}_0]} = \frac{(r_1 + r_2)r_3 + r_1(f_2 - \rho)}{(f_1 + l - \rho)(r_3 + f_2 - \rho)} e^{-\rho t} + \frac{e^{-(f_1+l)t}}{r_1r_3(f_1 + l - \rho) - [(r_1 + r_2)r_3 + r_1(f_2 - \rho)](f_1 + l - r_3 - f_2)} - \frac{r_1r_3}{(f_1 + l - r_3 - f_2)(r_3 + f_2 - \rho)} e^{-(r_3+f_2)t} \quad (10)$$

If f_2 , r_3 , and their sum are large,

$$\frac{B}{[\text{OX}_0]} = \frac{(r_1 + r_2)r_3 + r_1f_2}{(f_1 + l - \rho)(r_3 + f_2)} e^{-\rho t} + e^{-(f_1+l)t} \left\{ \frac{r_1r_3(f_1 + l - \rho) + [(r_1 + r_2)r_3 + r_1f_2](r_3 + f_2)}{-(r_3 + f_2)(f_1 + l - \rho)(r_3 + f_2)} \right\} \quad (11)$$

$$\frac{B}{[\text{OX}_0]} = \left\{ (r_1 + r_2) \frac{r_3}{r_3 + f_2} + \frac{r_1f_2}{r_3 + f_2} \right\} \frac{1}{f_1 + l - \rho} e^{-\rho t} - e^{-(f_1+l)t} \left\{ \frac{(r_1 + r_2)r_3}{(r_3 + f_2)(f_1 + l - \rho)} + \frac{r_1f_2}{(r_3 + f_2)(f_1 + l - \rho)} \right\} \quad (12)$$

$$\frac{B}{[\text{OX}_0]} = \frac{(r_1 + r_2) \frac{r_3}{r_3 + f_2} + r_1 \frac{f_2}{r_3 + f_2}}{(f_1 + l) - \rho} \{e^{-\rho t} - e^{-(f_1+l)t}\} \quad (13)$$

$$\frac{B}{[\text{OX}_0]} = \frac{r_1 + \frac{r_2r_3}{r_3 + f_2}}{(f_1 + l) - \rho} \{e^{-\rho t} - e^{-(f_1+l)t}\} \quad (14)$$

$$B = \frac{[\text{OX}_0] \left(r_1 + \frac{r_2r_3}{r_3 + f_2} \right)}{(f_1 + l) - \rho} \{e^{-\rho t} - e^{-(f_1+l)t}\} \quad (15)$$

$$I_t = \frac{d(h\nu)}{dt} = \Phi_f B \left(\frac{\Phi_f q}{m + q} \right) \quad (16)$$

But,

$$I_t = \frac{Mr}{f-r} \{e^{-rt} - e^{-ft}\} \quad (1)$$

$$I_t = \frac{\left(\frac{l\Phi_f q}{m+q} \right) [\text{OX}_0] \left(r_1 + \frac{r_2r_3}{r_3 + f_2} \right)}{(f_1 + l) - \rho} \{e^{-\rho t} - e^{-(f_1+l)t}\} \quad (17)$$

$$M = \Phi_f \frac{lq}{m+q} \left(r_1 + \frac{r_2r_3}{r_3 + f_2} \right) [\text{OX}_0] \quad (18)$$

At initial time, $t = 0$,

$$I_t(t=0) = \frac{Mr}{f-r} (1 - rt - 1 + ft) = Mrt \quad (19)$$

Let r be very large,

$$I = \frac{Mr}{-r} (-e^{-ft}) = Me^{-ft} \quad (20)$$

$$M = [\text{OX}_0] \left\{ \frac{lq\Phi_f}{m+q} \right\}$$

$$r = r_1 + r_2$$

$$\frac{M}{r} = [\text{OX}_0] \left\{ \frac{lq\Phi_f}{m+q} \right\} \left\{ \frac{r_1 + r_2 \left(\frac{r_3}{r_3 + f_2} \right)}{r_1 + r_2} \right\}$$

if $r_3 > f_2$

$$\frac{M}{r} \rightarrow [\text{OX}_0] \frac{lq\Phi_f}{m+q}$$

if $f_2 \gg r_3$

$$\frac{M}{r} \rightarrow \frac{[\text{OX}_0]lq\Phi_f}{m+q} \frac{r_1}{r_1 + r_2}$$